

Development of tissue scaffolds using selective laser sintering of polyvinyl alcohol/hydroxyapatite biocomposite for craniofacial and joint defects

C. K. CHUA*, K. F. LEONG, K. H. TAN, F. E. WIRIA, C. M. CHEAH

Rapid Prototyping Research Laboratory, School of Mechanical and Production Engineering, Nanyang Technological University, Singapore 639798

E-mail: mckchua@ntu.edu.sg

The growing interest in scaffold-guided tissue engineering (TE) to guide and support cell proliferation in the repair and replacement of craniofacial and joint defects gave rise to the quest for a precise technique to create such scaffolds. Conventional manual-based fabrication techniques have several limitations such as the lack of reproducibility and precision. Rapid prototyping (RP) has been identified as a promising technique capable of building complex objects with pre-defined macro- and microstructures. The research focussed on the viability of using the selective laser sintering (SLS) RP technique for creating TE scaffolds. A biocomposite blend comprising of polyvinyl alcohol (PVA) and hydroxyapatite (HA) was used in SLS to study the feasibility of the blend to develop scaffolds. The biocomposite blends obtained via spray-drying technique and physical blending were subjected to laser-sintering to produce test specimens. The SLS-fabricated test specimens were characterized using scanning electron microscopy and X-ray diffraction. The test specimens were also tested for bioactivity by immersing the samples in simulated body fluid environment. The results obtained ascertained that SLS-fabricated scaffolds have good potential for TE applications.

© 2004 Kluwer Academic Publishers

1. Introduction

The advent of tissue engineering (TE) has provoked the idea of being able to grow certain functional tissues to replace damaged, injured or worn parts of the human body. This vast interest generated among clinicians as well as engineers seeking for living replacements to rapidly and effectively treat malfunctioned human tissues and organs is incited by the immense potential and promise in overcoming the severe shortage of donor organs and the limitations of alternative short-term therapies (e.g. drugs, electro-mechanical prosthetics) [1–3].

Among the many critical issues that have to be addressed in TE, one challenge is to provide and optimize the use of TE scaffolds for directing and growing normal and healthy tissues. In the area of bioengineering and biomaterial sciences, the challenge is to create scaffolds that possess anatomically-accurate geometries and spatially controlled microstructures that would establish the necessary micro-environments required for cell proliferation, propagation and finally differentiation into functional components in an orchestrated TE construct [4–8]. To overcome the limitations such as irregularly shaped pores and the lack of spatial

control in current manual-based scaffold fabrication techniques [8,9], automated computer-controlled fabrication techniques, such as rapid prototyping (RP), are being explored [10–13]. Literature detailing some of the work carried out using RP techniques for creating TE scaffold is available elsewhere [14,15].

The application of selective laser sintering (SLS) [16] RP technique in fabricating scaffolds remains limited as commercially available SLS modeling materials are non-biocompatible. Research carried out using SLS for implant fabrication often involves the coating of HA powder with polymeric binders [17,18]. The SLS-fabricated implants are subsequently subjected to a two-step debinding and sintering process for binder removal and consolidation of the ceramic structure. These additional post-processing steps increases both the lead time and cost required in scaffold production. In addition, the use of organic solvents in the preparation process is not desirable as any residual traces of the solvent left behind may elicit inflammatory responses *in vivo*. The research work presented in this paper circumvents the use of such organic solvents by coating hydroxyapatite (HA) with a water-soluble polymer, polyvinyl alcohol (PVA), via spray drying technique

*Author to whom all correspondence should be addressed. Present address: 50 Nanyang Avenue, School of Mechanical and Production Engineering, Nanyang Technological University, Singapore 639798.

and physically blending mixtures of PVA and HA powder. The feasibility of sintering such powder blends and the influence of SLS process parameters on the sintering quality and the resulting microstructure of the sintered specimens were studied.

PVA has been used extensively in the treatment of defects in load-bearing joints such as cartilages due to its relatively similar tensile strength to human articular cartilage and its good lubrication [19–21]. In addition, the ability of PVA to form complex shapes with suitable adhesion makes it one of the ideal materials to treat complex craniofacial defects. Conventional cranioplasty often involves the usage of either HA or HA cement in the healing of craniofacial bone defects [22–24]. The approach taken by the team was aimed at creating an effective osseoconductive scaffold for bone replacement by taking advantage of the ability of SLS to fabricate complex shapes using PVA and the incorporation of HA into the PVA matrix to promote the ingrowth of bone cells.

2. Materials and methods

2.1. PVA and HA powder

Polyvinyl alcohol is a biodegradable, biocompatible and bioinert semi-crystalline copolymer of vinyl alcohol and vinyl acetate. The melting temperature, T_m , and glass-transition temperature, T_g , of PVA depend on the degree of cross-linking. Its T_m ranges from 220 to 240 °C and its T_g ranges from 58 to 85 °C for partially and fully hydrolyzed PVA, respectively; but it decreases in the presence of water [25]. Furthermore, the degradation period of PVA can be altered accordingly to suit the various TE applications making PVA an ideal material in the fabrication of TE scaffolds [26,27]. Pure PVA powder (99% + hydrolyzed, average molecular weight of 89 000–98 000) was obtained from Aldrich Chemical Company, Inc.

For the past decade, implants have been directed towards the use of bioactive fixation, in which interfacial bonding between the implant and tissue is generated from formation of a layer of biologically active material on the implant surface [28,29]. Hydroxyapatite is classified as a bioactive material that exhibits osteoconductivity. Thus, it forms a bioactive bond to bone with a strength equal to, if not greater than, bones that are 3–6 month-old. This high strength can be attributed to the *in vivo* growth of a dense layer of hydroxy-carbonate apatite (HCA) crystal agglomerates, which binds to collagen fibrils in bone structure. Apart from that, the use of HA also increases collagen production and enhances cellular response to the biomimetic structure.

There were two types of HA used in this research. The first type was in house HA powder, produced via a spray drying technique, in a manner that will be described later. The second is commercially available HA powder sold under the brand name CAMCERAM II HA (Cam Implants BV, Netherlands). This HA powder meets the ASTM F 1185–88 requirements and has a particle size distribution with at least 90 weight percentage below 60 µm, as determined by Coulter Counter analysis. The average material density is specified as 3.05 g/cm³.

2.2. Preparation of PVA and HA biocomposite

Two approaches were taken in the preparation of the biocomposite, namely spray drying and physical blending. In the first approach, the composite comprising of 70 weight percentage (wt %) spray-dried HA and 30 wt % PVA was obtained for laser-sintering via spray drying technique, in which the spray-dried HA powder was coated with PVA. Spray-dried HA was produced in house via direct precipitation reaction of calcium hydroxide (Merck) and ortho-phosphoric acid 85% (Merck) in which the suspension was spray-dried using a spray dryer (Ohkawara Kakohki Co. Ltd., Model L-12) to obtain the HA powder. This in house spray-dried HA powder was then diluted in distilled water to get the spray-dried HA suspension. Subsequently, the PVA powder was slowly added to heated distilled water and the solution was continuously stirred to ensure a homogenous solution. The dissolution rate decreases as the concentration of dissolved PVA in the distilled water increases. Therefore, complete dissolution of PVA in the distilled water had to be ensured. When the PVA granules were completely dissolved, the PVA solution was slowly poured into the pre-prepared spray-dried HA suspension while continuously stirring the suspension. As the presence of PVA in the suspension resulted in a viscous suspension, tending to settle down causing a non-uniform mixture, the suspension needed to be manually stirred every 15 min. In addition, it was noted that for every 9 liters of spray-dried HA/PVA suspension, the yield of spray-drying HA/PVA biocomposite powder was between 150 and 200 g.

In the second approach, pure Camceram HA powder was physically blended with pure PVA powder. In producing the blends, PVA was the base material and HA was added and dispersed into the PVA powder to achieve powder blends having 10, 20 and 30 wt % HA contents. The polymer blend was put on a mixing roller (US Stoneware, East Palastine, OH 44413). The rollers were run for 3 h at 40 rpm. These values were selected, as they were considered sufficient to ensure thorough mixing of the blend [30].

2.3. Design and fabrication of test specimens

The test sintering of the biocomposite material was done by sintering a thin circular disc with diameter and thickness of 16 and 0.762 mm, respectively for microscopic examination and bioactivity assessments. The test specimen was purposely designed to have a diameter of 16 mm to ensure that the specimens fit into a standard 24-well cell culture plate snugly. The CAD model of the test specimen was generated using a standard CAD software, ProENGINEER Ver. 2000i (Parametric Technology Corp., Needham, MA) and exported in the .STL file format for uploading into the SLS system.

Test specimens of the spray-dried biocomposite and the prepared powder blends were processed on a commercial SLS system, Sinterstation 2500 (3D Systems Inc., Valencia, CA). Except for changing the process parameters on the operating software of the SLS

TABLE I Specimen groups for pure PVA, spray-dried and physically blended PVA/HA biocomposite powder

| Laser power (W) | Scan speed | | |
|-----------------|---|---|--|
| | Pure PVA (mm/s (in/s)) | Spray-dried PVA/HA (mm/s (in/s)) | Physically blended PVA/HA (mm/s (in/s)) |
| 3 | <p style="text-align: center;">↑</p> <p style="text-align: center;">1270 (50)</p> <p style="text-align: center;">1778 (70)</p> <p style="text-align: center;">2540 (100)</p> <p style="text-align: center;">5080 (200)</p> <p style="text-align: center;">↓</p> | <p style="text-align: center;">↑</p> <p style="text-align: center;">1270 (50)</p> <p style="text-align: center;">1778 (70)</p> <p style="text-align: center;">↓</p> | |
| 4 | | | |
| 5 | | | |
| 6 | | | |
| 7 | | | |
| 8 | | | |
| 9 | | | |
| 10 | | | |
| 11 | | | |
| 12 | | | |
| 13 | | | |
| 14 | | | |
| 15 | | | 1270 (50) 1778 (70) |
| 16 | | | |
| 17 | | 1016 (40) 5080 (200) | |
| 18 | | | |
| 19 | | | |
| 20 | | | |

system, no other modifications were made on the SLS system for processing the new materials.

Experiments were carried out to obtain the optimal parameters of SLS and composition of biocomposite for successful fabrication. The influence of the two main SLS process parameters, namely laser power and scan speed, on the degree of sintering of pure PVA was firstly investigated.

The settings for the SLS process parameters were kept at their default values except for laser power and scan speed, which were set initially at 3 W and 5080 mm/s (200 in/s) respectively. The part bed temperature was set at 65 °C, which is close to T_g of PVA. Pure PVA was then subjected to laser-sintering at different laser powers and scan speeds to determine the optimal settings for its sintering. By varying the two process parameters, five groups of specimens comprising different blends of PVA and HA, were fabricated. The five groups were pure PVA powder, spray-dried PVA/HA biocomposite and physically blended PVA/HA biocomposite consisting of 10 wt %, 20 wt % and 30 wt % of HA. Table I shows the various parameter settings on SLS for fabricating the various test specimens.

2.4. Characterization of test specimens

Pure powders and test specimens were observed by scanning electron microscopy (SEM), JEOL JSM-5600 LV, to determine the surface morphology and microstructure of the sintered specimens. X-ray diffraction (XRD) technique, Philips PW 1830 X-ray diffractometer, was used to identify and determine the various phases of compounds present in both the powdered and solid samples. The XRD tests were conducted using step scan in which the angle (2θ) was set between 10° and 80°, step size at 0.02° and time per step of 1 s.

Bioactivity testing of the sintered biocomposite was conducted by immersing the specimens in simulated body fluids (SBF), which is a solution that has ion concentration and pH similar to those of human blood

plasma. As HA is a bioactive material, it is natural for HA to exhibit a biologically active layer after implantation to establish bonding with bone. Thus it is crucial for the PVA/HA specimens to be able to induce this aforementioned layer *in vitro*. Test specimens were soaked in SBF for two weeks at 36.5 °C, changing the solution every two days. Whenever the solution was changed, a sample was retrieved for characterization by SEM or XRD.

3. Results and discussion

3.1. Microscopic examination of powder stocks

Microscopic examinations were carried out on the as-received powder stocks and the biocomposite powder after spray drying and blending. The results of the examinations are presented in the following sections.

3.1.1. Raw powder stocks

Fig. 1(a)–(c) are micrographs of the as-received PVA, as-received HA and spray-dried HA powder, respectively. As observed in these figures, the PVA powder are spherical in shape with irregular surface texture (average particle size approximately 50–100 μm) compared to the spherical HA powder with smooth surface texture (average particle size less than 60 μm). This distinct morphological feature between the two materials made the identification of HA particles in the sintered PVA matrix much simpler.

3.1.2. Spray-dried PVA/HA powder prior to laser sintering

Fig. 2 shows the micrograph taken for the spray-dried PVA/HA composite prior to laser-sintering. The larger sized powder is identified to be PVA particles whereas the smaller ones are HA particles. It was observed that the spray-drying method resulted in HA particles coated

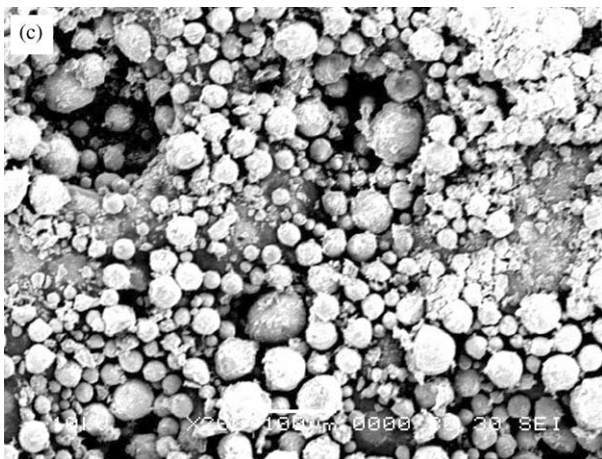
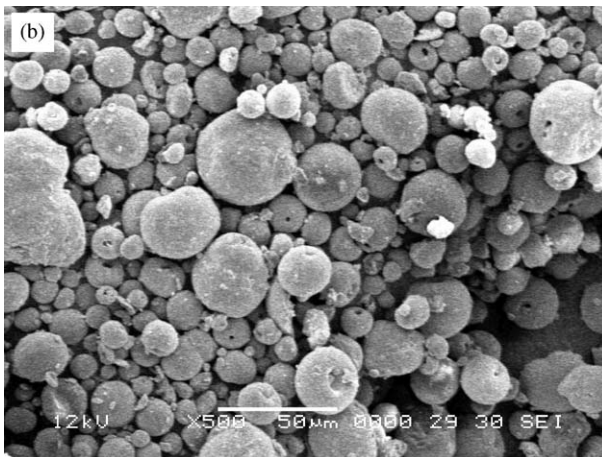
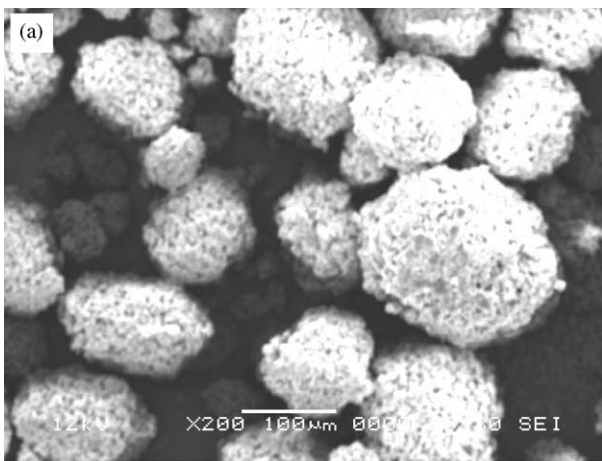


Figure 1 Micrographs taken for the (a) as-received PVA, (b) as-received HA powder and (c) spray-dried HA powder.

by PVA particles as circled in Fig. 2 in a random manner. However, since composition of PVA : HA was 30 : 70 by weight, it was noted that there were more HA particles than PVA and the HA particles were left either unattached to the PVA particles (as boxed), or sticking to the biocomposite particles.

3.1.3. PVA/HA powder blends prior to laser sintering

Fig. 3(a)–(c) present the micrographs taken for the three different powder blends containing 10–30 wt % HA respectively prior to laser sintering.

HA particles (as circled) in all three different powder blends were observed to have increasing amounts with increased weight percentage of HA content in the biocomposite. It is worthwhile to note that regardless of the composition, SEM observation of the HA particles on all samples indicates that mixtures with good dispersion and distribution of HA were obtained.

3.2. Optimization of SLS parameters

Prior to experimenting with PVA/HA biocomposite powder, pure PVA powder was test-sintered. The aim was to establish a set of suitable processing parameters for processing thereafter the biocomposite powder. Attempts to sinter pure PVA powder at part bed temperature lower than 65 °C with a default scan speed of 5080 mm/s (200 in/s) yielded specimens that exhibited limited sintering effect. The resulting specimens were too weak to be handled manually. It was also noted that a difference in laser power of 4 W and below did not give a highly significant variance of sintering result. However, at laser powers above 20 W, the powder actually flamed up and hence the highest laser power used was 15 W. With these observations, the scan speed was lowered to 2540 mm/s (100 in/s) and the part bed temperature was set at 65 °C. Fig. 4(a) and (b) shows the sintering result of pure PVA sintered at a constant part bed temperature of 65 °C and scan speed of 2540 mm/s (100 in/s). Efforts to laser-sinter pure PVA powder at laser power lower than 13 W were not successful. “Necking” between particles, a phenomenon of sintering, was noted in the specimens laser-sintered at 13 W and above as circled in Fig. 4(a) and (b). Although there was sintering effect at 2540 mm/s (100 in/s) and 15 W, it was observed that the test specimens changed color from white (color of the PVA powder) to brownish indicating possible charring. However, the test specimen did not flame during the processing.

According to the Andrew’s number theory, the energy density received by the powder in a specimen is directly proportional to the laser power and inversely proportional to the scan speed [31, 32]. Since the energy density affects the degree of sintering of the exposed powder, specimens with different porosity can be obtained by

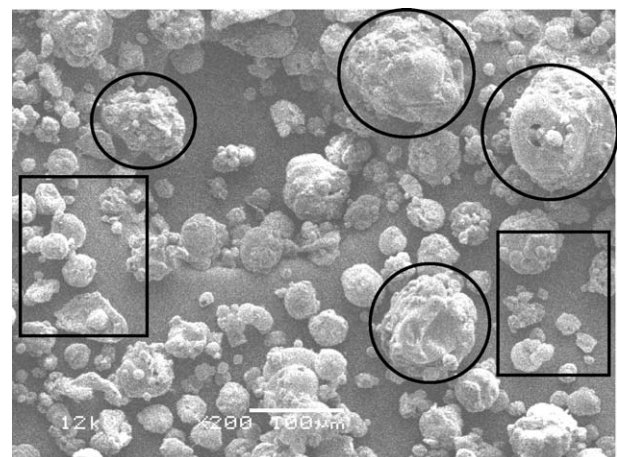


Figure 2 Micrographs taken for spray-dried PVA/HA biocomposite magnified 200 times.

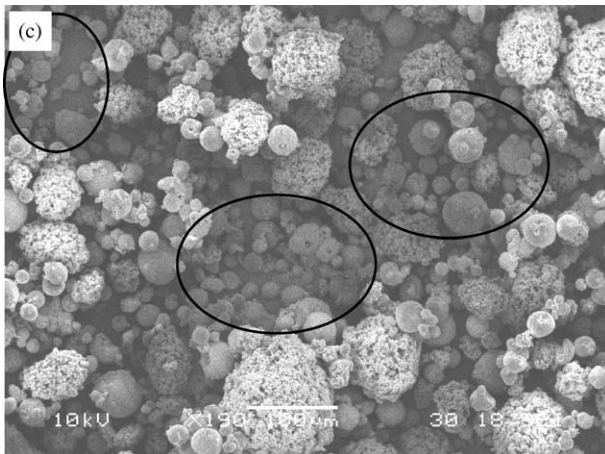
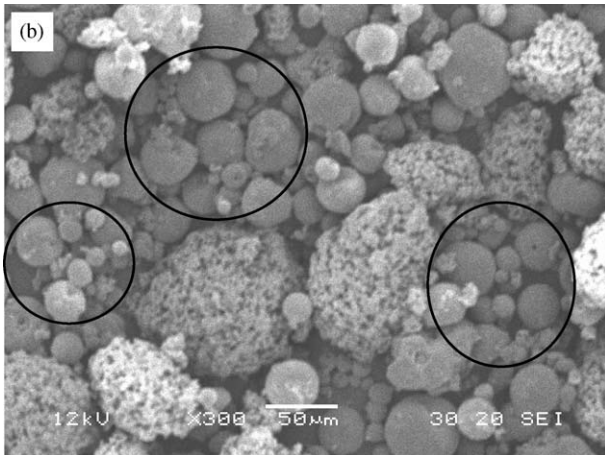
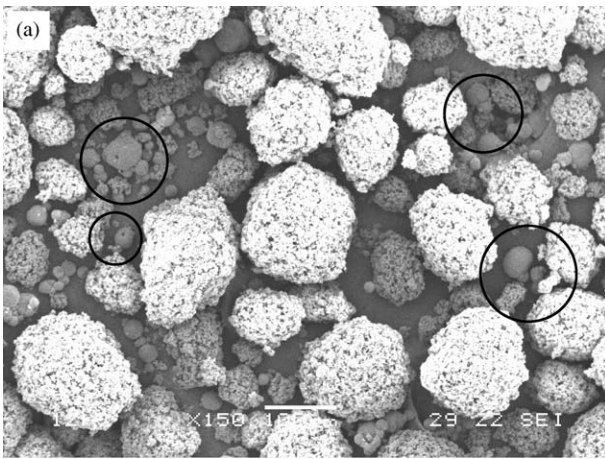


Figure 3 Micrograph of PVA/HA powder blend before sintering for different weight composition: (a) 10 wt% HA, (b) 20 wt% HA and (c) 30 wt% HA.

varying these SLS process parameters. Therefore, to obtain the same energy density in the test specimens, the scan speed was decreased and the laser power was increased to study the sintering effect. As delamination (edges opening up) was observed at laser power lower than 10 W, the laser power was gradually increased to 15 W for both scan speed of 1270 mm/s (50 in/s) and 1778 mm/s (70 in/s). Promising result of structurally stable specimens was observed from 13 W at 1778 mm/s (70 in/s) to 10 W at 1270 mm/s (50 in/s). Fig. 5(a) and (b) illustrate the sintering results of pure PVA specimens laser-sintered at these two sets of parameters. No significant differences in the sintering result between the two micrographs were observed. Attempts to sinter

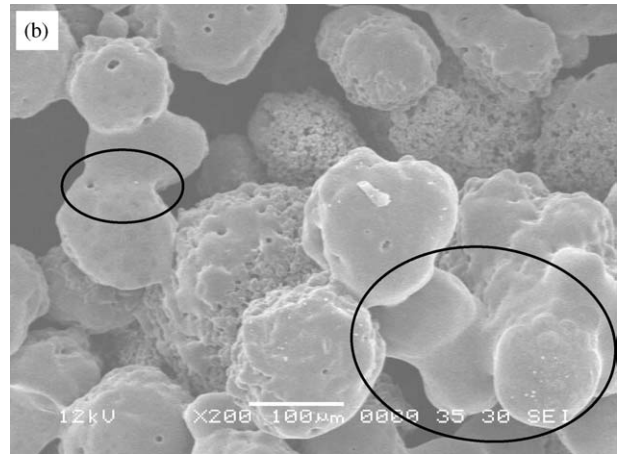
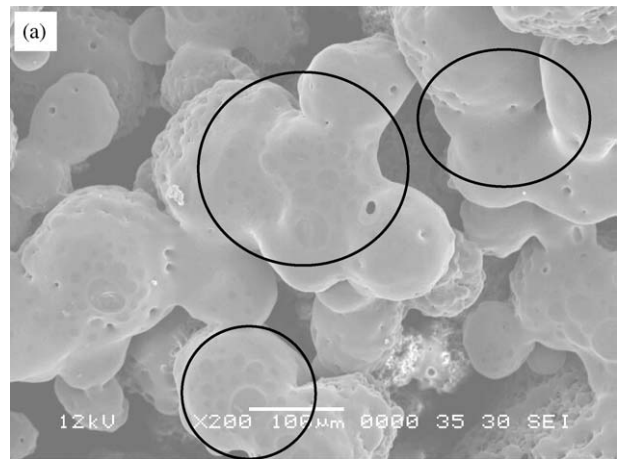


Figure 4 Micrograph of sintered pure PVA specimens produced at 2540 mm/s(100 in/s) and laser power settings of: (a) 13 W and (b) 15 W.

pure PVA at 1270 mm/s (50 in/s) and 16 W resulted in the flaming of the specimens suggesting that the combination of low scan speed and high laser power led to excessive energy density in the test specimens. Therefore, it is concluded that the suitable processing windows on SLS were 13–15 W for the laser power and 1270 mm/s (50 in/s) to 1778 mm/s (70 in/s) for the scan speed. However, for standardization in this paper, the laser power was set at 15 W and scan speed at 1270 mm/s (50 in/s) for laser-sintering the spray-dried and physically blended PVA/HA biocomposite for comparison.

3.3. Laser-sintering of spray-dried PVA/HA biocomposite powder

The spray-dried PVA/HA powder was fabricated according to the parameters in the previous section. Test specimens fabricated appeared very fragile as if there were limited fusing between the powder particles. The fragility of the specimens made the manual handling of the test specimens almost impossible and examination under SEM revealed no ‘‘necking’’ between the particles even at high magnification. Efforts to further increase the laser power resulted in flaming during the fabrication process, hence making it impossible to fabricate any test specimens. As the relatively low scan speed of 1270 mm/s (50 in/s) did not yield any specimen that could be handled, the spray-dried PVA/HA composite may not be feasible for fabrication on the SLS. The

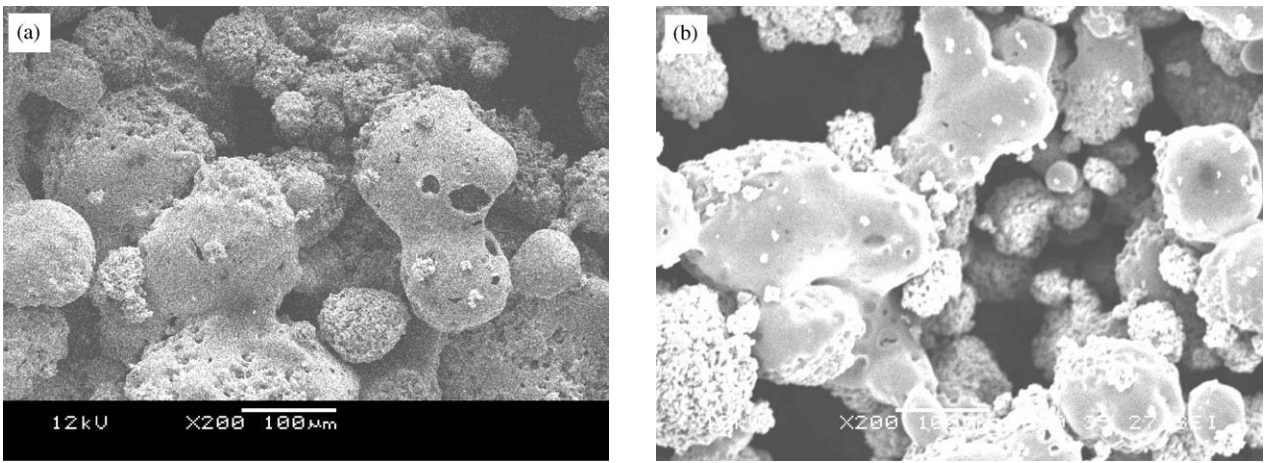


Figure 5 Micrograph of sintered pure PVA specimens produced at scan speed of: (a) 1778 mm/s(70 in/s) with laser power of 13 W and (b) 1270 mm/s(50 in/s) with laser power of 10 W.

unsuccessful sintering on SLS was likely due to the fact that there was too much HA in the composition and hence the PVA as a binder could not hold the test specimens strongly together. Therefore, in order to yield successful sintering, a higher weight percentage of PVA could be used in the spray-drying process. However, it should be noted that the spray-drying technique to produce the biocomposite gives rise to two main problems. First, the yield of powder from spray drying did not justify the large amount of slurry that was needed (see Section 2.2) and hence this was a labor-intensive preparation process. The second problem was that with this method it is impossible to distinguish between the PVA and HA particles within the composite powder. Due

to these two problems, it was decided to physically blend the powders before laser-sintering.

3.4. Laser-sintering of physically blended PVA/HA biocomposite powder

Fig. 6(a)–(c) show the micrographs for different composition of sintered PVA/HA polymer blend fabricated at laser power of 15 W and scan speed of 1270 mm/s (50 in/s).

As observed in Fig. 6, prominent sintering effect exhibiting well-defined micro pore interconnectivity can be seen in all micrographs. In addition, the HA particles

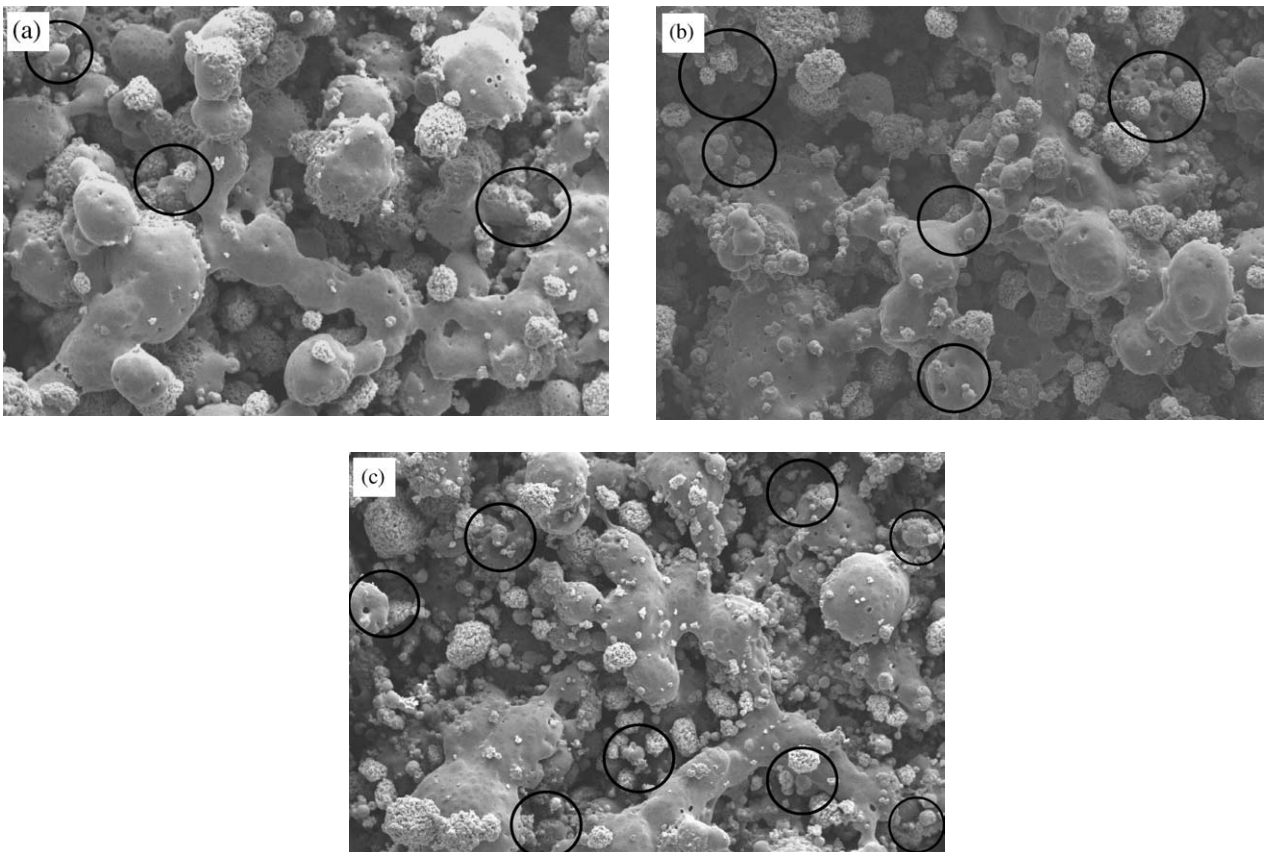


Figure 6 Micrographs of sintered PVA/HA polymer blend with: (a) 10 wt % HA, (b) 20 wt % HA and (c) 30 wt % HA, magnified 100 times.

(indicated by circles) were noted to have been well dispersed in the PVA matrix and have attached to the much larger PVA particles. The amount of HA embedded in the PVA matrix also increased with increasing weight percentage of HA used. It was noted that as the weight percentage of HA in the polymer blend increased, less sintering effects were noted as less PVA particles were fused together. This corresponds to the argument that PVA acts as the polymeric binder in the biocomposite polymer blend. Hence it is recommended that the weight percentage of HA be kept at 30 wt% to yield successful scaffold specimens with well-defined pore interconnectivity and good structural integrity. In addition, the exposure of HA in the PVA matrix would encourage the proliferation of osteoblast cells after the scaffolds are implanted. The successful sintering of the test specimens indicated the potential of producing PVA scaffolds with SLS. Furthermore, the successful incorporation of HA into the polymer matrix will enhance the bioactivity of the specimens in treating craniofacial and joint defects.

3.5. Bioactivity analysis using SBF

The fabricated test specimens from physically blended PVA/HA powder were subjected to bioactivity analysis using SBF. As this was done to assess the influence of HA, only test specimens comprising 90 wt% PVA and 10 wt% HA would be sufficient for this bioactivity analysis. Fig. 7 shows the test specimens after immersion in SBF.

Visual observations on 3rd and 5th day showed that the test specimens had swollen. PVA, being a water-soluble hydrogel, it would swell in the presence of the fluid. Therefore samples were difficult to handle. Upon drying, the samples shrank back to their original size. As shown in Fig. 7(a) and (b), there was a change in the surface appearance of the specimen, which looked very different from Fig. 6. This unique layer was usually located at isolated spots of the sample. With a very high SEM magnification of 1000 times, it was observed that this layer was likely to be hydroxy-carbonate apatite (HCA), which is normally found when HA is soaked in SBF environment [33, 34]. Formation of HCA is because there is an ion exchange between HA in the PVA matrix and SBF [34, 35]. Carbonates (CO_3^{2-}) from SBF would eventually substitute phosphate (PO_4^{3-}) in the HA to form HCA. The presence of HA in Fig. 7(a)–(c) is indicated by the rectangular blocks. They show the individual HA particles precipitating to become HCA. When the test specimens were soaked in SBF for more than 9 days, some HA particles seemed to float in the SBF and some of the HA particles had deposited at the bottom of the specimens. This phenomenon was further verified by SEM inspection of the 9th day-specimen. Fig. 7(c) shows that although the thickening of the layer existed, it was very scarce and only found at isolated spots using very high magnification, indicating the possibility of HA powder falling off the sample and hence no significant HCA layer was present. As the samples swelled in the SBF environment and shrank upon drying, the bond between sintered PVA and HA might loosen and hence HA particles may have been

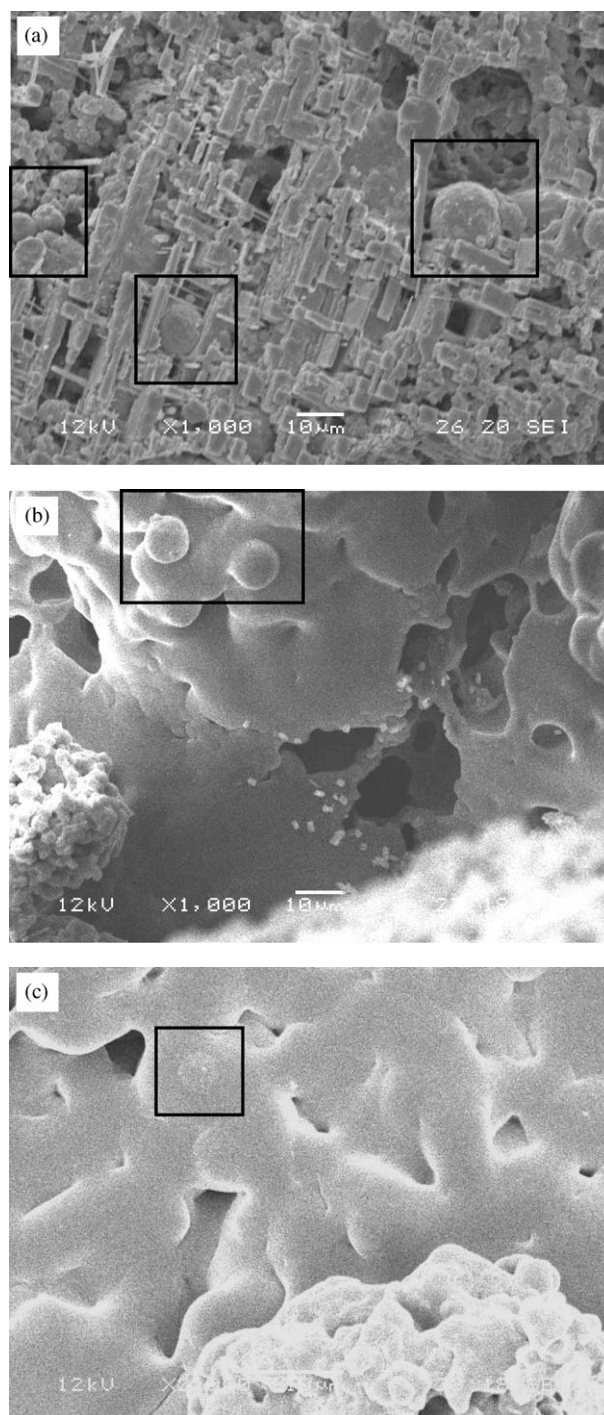


Figure 7 Micrographs of test specimens after immersion in SBF on: (a) 3rd day, (b) 5th day and (c) 9th day, magnified for 1000 times.

dislodged from the specimens. Therefore X-ray diffraction (XRD) was used to verify this observation.

In XRD analysis, normally three highest peaks of a material must be identified to ensure that the material is composed of the correct substances. Fig. 8 shows the XRD comparison of pure PVA powder, PVA/HA biocomposite with 10 wt% HA and test specimen after immersion in SBF for 14 days.

Presence of PVA in the PVA/HA biocomposite with 10 wt% HA and test specimen after immersion in SBF for 14 days can be identified by comparing the peaks in pure PVA powder respectively. The peaks occurred at 2θ angle of 11.48° , 19.44° , 22.18° and 43.5° , as shown by the rectangular blocks. HA's peak in the PVA/HA biocomposite with 10 wt% HA and test specimen after

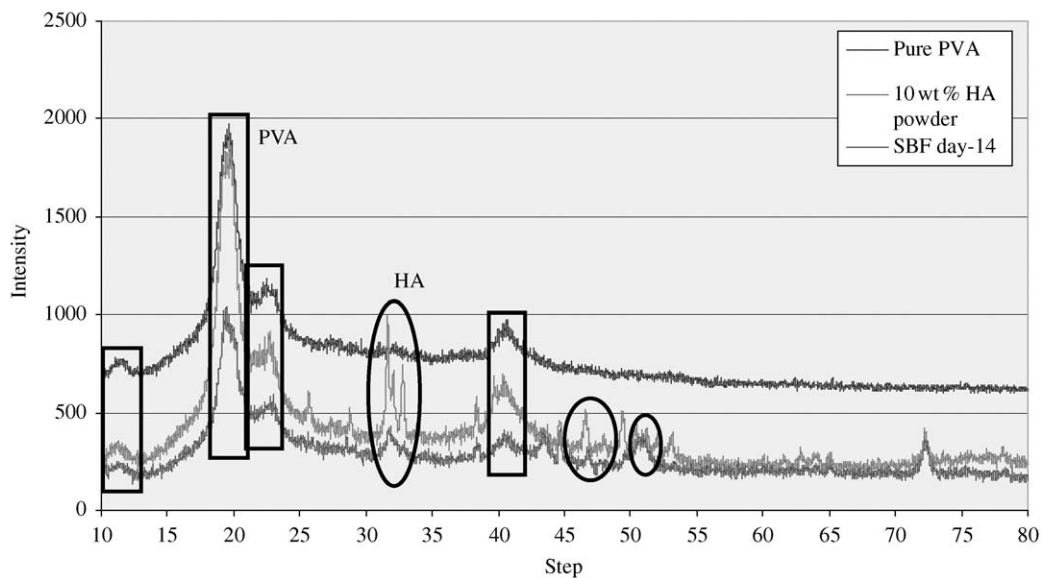


Figure 8 XRD comparison of pure PVA, PVA/HA biocomposite with 10 wt % HA and test specimen after immersion in SBF for 14 days.

immersion in SBF for 14 days was identified with reference to the Joint Committee of Powder Diffraction Standard (JDCPS) reference card no. 9-0432 for calcium phosphate hydroxide. It can be seen that there are four highest peaks of HA, as circled, located at 2θ angle of 31.66° , 32.76° , 46.72° and 50.5° . These HA peaks also occurred at the same or nearby angle 2θ of 14th day SBF sample. Presence of HCA in the SBF sample were identified by HA peaks, as HCA was precipitated from HA in the presence of SBF. Therefore HCA and HA should have peaks at the same location. Since reaction of test specimen in the SBF environment has made slight dissolution of PVA and HA, it should be noted that PVA and HA peaks that occurred in the SBF sample were not as sharp as when they occurred in pure PVA or PVA/HA biocomposite with 10 wt % HA. The bioactivity analysis has confirmed the presence of HA particles in the PVA matrix and hence ascertained that the physically blended processing technique did not prevent the incorporation of HA into the PVA matrix.

4. Conclusion

The research explored the potential of using RP technology to replace the conventional techniques for fabricating TE scaffolds, which are not versatile to meet the various aspects required for TE scaffolds. RP technology, in particular SLS, was investigated to bridge the gap left behind by conventional techniques. Utilizing PVA and HA as biomaterials, research was carried out to develop a biocomposite powder system. The result has shown that physically blended powders yielded test specimens that exhibited good micropore interconnectivity and reproducibility. Bioactivity tests of specimens using SBF showed that laser-sintering did not affect the chemical composition of HA in the PVA matrix, as the HA was still bioactive in the SBF environment. The SBF experiments thus indicated the compatibility of sintered PVA/HA blend in human body fluid environment by the precipitation of the apatite layer on the specimens. The aforementioned results have ascertained the viability of using the PVA/HA blend as

base material in fabricating TE scaffolds on SLS in the treatment of bone defects with the successful incorporation of bioactive HA into the test specimens.

Acknowledgments

The authors would like to acknowledge Associate Professor Philip Cheang (Director, Advanced Materials Research Centre) at School of Material Engineering in Nanyang Technological University for providing the usage of the facilities and support in the materials used in this research.

References

1. L. G. GRIFFITH and G. NAUGHTON, *Science* **295** (2002) 1009.
2. E. BELL, in "Principles of Tissue Engineering", 2nd edn, edited by R. P. Lanza, R. S. Langer and J. P. Vacanti (Academic Press, London, 2000).
3. D. J. MOONEY and A. G. MIKOS, *Scientific American*, April (1999).
4. K. WHANG, K. E. HEALY, D. R. ELENZ, E. K. NAM, D. C. TSAI, C. H. THOMAS, G. W. NUBER, F. H. GLORIEUX, R. TRAVERS and S. M. SPRAGUE, *Tissue Eng.* **5** (1999) 35.
5. W. S. KIM, J. P. VACANTI, L. CIMA, D. MOONEY, J. UPTON, W. C. PUELACHER and C. A. VACANTI, *Plastic Reconstr. Surg.* **94** (1994) 233.
6. M. W. DAVIES and J. P. VACANTI, *Biomaterials* **17** (1996) 365.
7. L. E. NIKLASON, J. GAO, W. M. ABBOTT, K. HIRSCHI, S. HOUSER, R. MARINI and R. LANGER, *Science* **284** (1999) 489.
8. W. L. MURPHY, R. G. DENNIS, J. L. KILENY and D. J. MOONEY, *Tissue Eng.* **8** (2002) 43.
9. A. G. MIKOS, Y. BAO, L. G. CIMA, D. E. INGBER, J. P. VACANTI and R. LANGER, *J. Biomed. Mater. Res.* **27** (1993) 183.
10. S. LIMPANUPHAP and B. DERBY, *J. Mater. Sci.: Mat. Med.* **13** (2002) 1163.
11. T. M. G. CHU, J. W. HALLORAN, S. J. HOLLISTER and S. E. FEINBERG, *ibid.* **12** (2001) 471.
12. S. BOSE, J. DARSELL, H. L. HOSICK, L. YANG, D. K. SARKAR and A. BANDYOPADHYAY, *ibid.* **13** (2002) 23.
13. K. H. TAN, C. K. CHUA, K. F. LEONG, C. M. CHEAH, P. CHEANG, M. S. ABU BAKAR and S. W. CHA, *Biomaterials* **24** (2003) 3115.
14. K. F. LEONG, C. M. CHEAH and C. K. CHUA, *ibid.* **24** (2003) 2363.

15. S. F. YANG, K. F. LEONG, Z. H. DU and C. K. CHUA, *Tissue Eng.* **8** (2002) 1.
16. C. K. CHUA, K. F. LEONG and C. S. LIM, in "Rapid Prototyping: Principles and Applications", 2nd edn (World Scientific, Singapore, 2003).
17. G. LEE, J. W. BARLOW, W. C. FOX and T. B. AUFDERMORTE in Proceedings of Solid Freeform Fabrication Symposium, Austin TX, August 12–14, 1996, p. 15.
18. N. K. VAIL, L. D. SWAIN, W. C. FOX, T. B. AUFDLEMORTE, G. LEE and J. W. BARLOW, *Mater. Design* **20** (1999) 123.
19. Y. S. CHANG, H. O. GU, M. KOBAYASHI and M. OKA, *The Knee* **5** (1998) 205.
20. M. OKA, K. USHIO, P. KUMAR, K. IKEUCHI, T. NAKAMURA and H. FUJITA, *J. Eng. Med.* **214** (2000) 59.
21. S. J. BRYANT, C. R. NUTTELMAN and K. S. ANSETH, *Biomed. Sci. Instrum.* **35** (1999) 309.
22. P. C. HOBAR, J. A. HUNT and S. ANTROBUS, *Plast Reconstr. Surg.* **111** (2003) 1667.
23. D. LEW, B. FARRELL, J. BARDACH and J. KELLER, *J. Oral. Maxillofac. Surg.* **55** (1997) 1441.
24. B. L. EPPLEY, *J. Craniofac. Surg.* **14** (2003) 85.
25. N. A. PEPPAS, in "Hydrogels in Medicine and Pharmacy. Volume II: Polymers", 2nd edn, edited by N. A. Peppas (CRC Press, Boca Raton, FL, USA, 2000) p. 16.
26. A. CORTI, R. SOLARO and E. CHIellini, *Polymer Degradation and Stability* **75** (2002) 447.
27. R. H. SCHMEDLEN, K. S. MASTERS and J. L. WEST, *Biomaterials* **23** (2002) 4325.
28. J. M. TABOAS, R. D. MADDOX, P. H. KREBSBACH and S. J. HOLLISTER, *ibid.* **24** (2003) 181.
29. T. H. ANG, F. S. A. SULTANA, D. W. HUTMACHER, Y. S. WONG, J. Y. H. FUH, X. M. MO, H. T. LOH, E. BURDET and S. H. TEOH, *Mater. Sci. Eng. C* **20** (2002) 35.
30. M. S. ABU BAKAR, M. H. W. CHENG, S. M. TANG, S. C. YU, K. LIAO, C. T. TAN, K. A. KHOR and P. CHEANG, *Biomaterials* **24** (2003) 2245.
31. K. F. LEONG, K. K. S. PHUA, C. K. CHUA, Z. H. DU and K. O. M. TEO, *J. Eng. Med.* **215** (2001) 191.
32. J. C. NELSON, Ph.D. Thesis, The University of Texas at Austin, USA (1993).
33. P. SIRIPHANNON, Y. KAMESHIMA, A. YASUMORI, K. OKADA and S. HAYASHI, *J. Biomed. Mater. Res.* **60** (2002) 175.
34. S. W. K. KWEH, K. A. KHOR and P. CHEANG, *Biomaterials* **23** (2002) 775.
35. E. KONTONASAKI, T. ZORBA, L. PAPADOPOULOU, E. PAVLIDOU, X. CHATZISTAVROU, K. PARASKEVOPOULOS and P. KOIDIS, *Cryst. Res. Technol.* **37** (2002) 1165.

*Received 3 June 2003
and accepted 18 March 2004*